Effect of In-Flight Ice Accretion on the Performance of a Multi-Element Airfoil

Abdollah Khodadoust
Chet Dominik
McDonnell Douglas Aerospace
Long Beach, CA 90810-1864

Jaiwon Shin
Dean Miller
NASA Lewis Research Center
Cleveland, OH 44135

Abstract

The effects of potential in-flight ice accretion on the aerodynamic performance of a multi-element high-lift airfoil have been investigated at moderate-to-high Reynolds numbers. The investigation was conducted in the Low Turbulence Pressure Tunnel (LTPT) at NASA Langley Research Center. Simulated ice shapes obtained from earlier testing in the Icing Research Tunnel (IRT) at NASA Lewis Research Center were used on all three elements of the multi-element configuration. Incremental performance effects due to the ice accretion are presented for both smooth and rough ice accretions. Reynolds number effects on the measured performance characteristics were also assessed. The present results confirm the importance of avoiding any ice accretions on the forward element of a lifting configuration.

NOMENCLATURE

α	angle of attack, degrees
δ_S	slat deflection angle, degrees
δ_F	flap deflection angle, degrees
C_p	pressure coefficient
k/c	ratio of roughness height to airfoil chord
M	free stream Mach number
$\Delta C_{\ell,max}$	loss in maximum lift coefficient
RN	Reynolds number based on chord
x/c	nondimensional coordinate
LTPT	Low Turbulence Pressure Tunnel
IRT	Icing Research Tunnel

Presented at the AHS/SAE International Icing Symposium '95, Montreal, Canada, September 18-21, 1995. *Copyright © by the American Helicopter Society, Inc. All rights reserved.*

INTRODUCTION

High-lift system improvements on tra aircraft have been the subject of extensive res for the past few years[1,2]. In order for the s systems to achieve high levels of performanc new designs are often highly optimized for ga overhang. As such, there was a concer environmental contamination, such as in-fli accretion, could cause a significant degrada the high-lift system's performance.

Performance of airfoils and win adverse weather conditions has been a sub investigation in the past[3-6]. Lynch et. documented the effects of leading edge rou on wings/airfoils in cruise and l configurations. Their measurements ind $\Delta C_{\ell,max}$ values over 30% were possible f cruise configuration and over 10% for the la configuration airfoils. The reduction in an attack margin to stall was as much as 5 degre both cruise and landing configurations. performance of a similar airfoil was tested takeoff configuration by Bragg et. al.[5] to asse

impact of underwing frost caused by cold-soaked fuel. Little change in the drag and maximum lift was noted when the frost formation was simulated downstream of the stagnation point (at maximum lift) on the main element. The effect of frost formation on the upper surface of an airfoil similar to that used above was evaluated by Valarezo[6]. The measurements indicated that in the takeoff configuration, maximum lift/stall-margin losses were most significant when the frost formation was simulated on the slat.

Most recently, the performance of an advanced technology high-lift airfoil was evaluated in the presence of in-flight ice accretion at moderate-to-high Reynolds numbers at NASA Langley's LTPT. The performance of the high-lift system was evaluated to determine incremental effects of ice. The results reported here are part of a cooperative experimental program conducted by McDonnell Douglas Aerospace, NASA Lewis Research Center, and NASA Langley Research Center to establish a data base of high-lift airfoil ice accretions and their effect on high-lift system performance.

TEST FACILITY AND MODEL DESCRIPTION

The Langley LTPT is a single return, closed throat wind tunnel that can be operated up to 10 atmospheres thus allowing very high Reynolds number capability[7] (Fig. 1). The test section is 3 feet wide by 7.5 feet high by 7.5 feet long. A sidewall boundary layer control (BLC) system in the test section is used to promote two-dimensional flow over the model. The BLC system uses the differential pressure between the test section and the atmosphere to provide suction of the boundary layer through porous endplates. The system yielded good quality two-dimensional flow over the model for the Reynolds numbers tested[8].

The model spanned the width of the test section and had a stowed airfoil chord of 22 inches. The multi-element airfoil tested in the landing configuration is shown in Fig. 2. The slat chord ratio was 14.48% and the flap chord ratio was 30% for both configurations tested. The slat and flap had deflections of 30-degrees with respect to the main element.

The multi-element airfoil was tested both in the clean and iced configurations. The iced configuration of the airfoil is shown in Fig. 2. The ice shapes tested were simulations of measurements taken in the NASA Lewis' IRT on a similar model[9,10]. Typical approach conditions for a narrow body twin-jet transport aircraft were used to simulate the flight-scale icing encounter in the IRT.

The roughness associated with the iced surfaces was simulated by applying carborandum grit particles on top of the smooth ice shapes on the slat, main element, and flap of the multi-element high lift airfoil. The appropriate "grit" size was estimated using a two-step process. First, the ice roughness size was estimated for a similar 3-foot chord multi-element high-lift airfoil which was tested in the NASA Lewis' IRT[9,10]. Second, this ice roughness height was geometrically scaled to be consistent with the LTPT high-lift airfoil. This scaled value of roughness size was used to select the appropriate grit sizes for the ice shapes on the slat, main element, and flap of the LTPT airfoil.

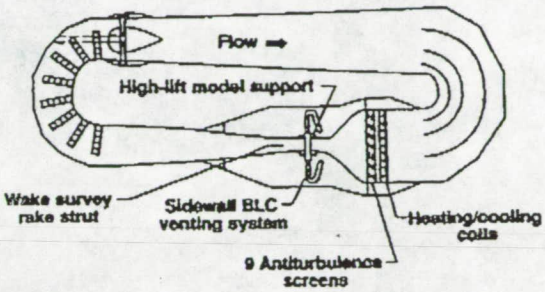

Fig. 1. Schematic of Low Turbulence Pressure Tunnel (LTPT)

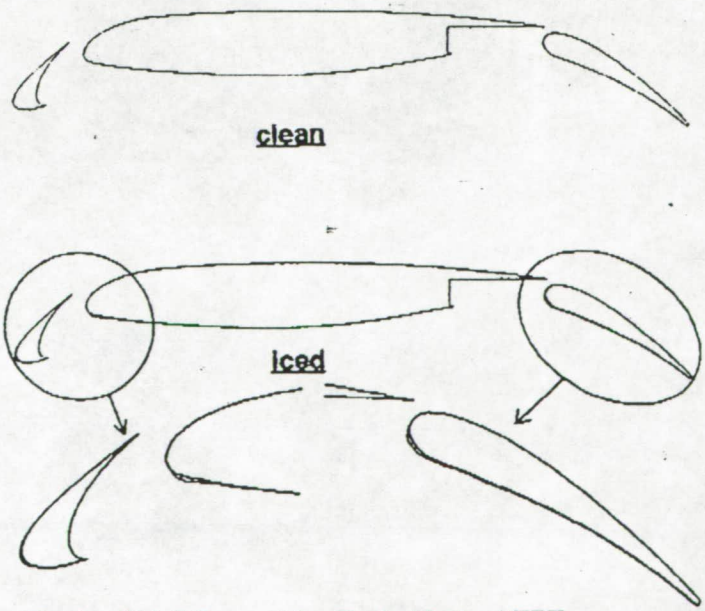

Fig. 2. Airfoil Geometries Tested in the LTPT

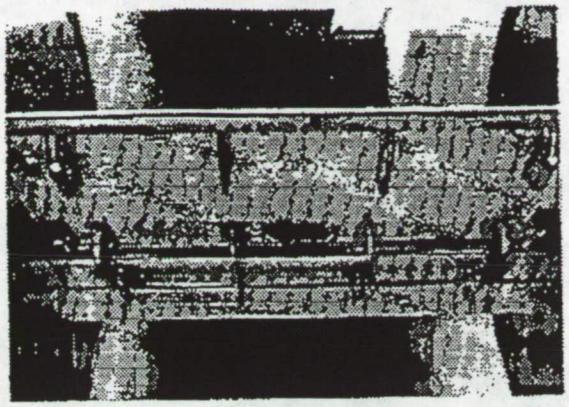

Fig. 3. View of High-Lift Model Support Brackets

Instrumentation consisted of pressure orifices located along the centerline of the model. The clean and iced slat each had 40 chordwise and 10 spanwise pressure orifices. The main element had 43 chordwise and 10 spanwise pressure orifices in each of the clean and iced configurations. The clean flap had 62 chordwise and 20 spanwise pressure orifices. The iced flaps had 49 chordwise and 20 spanwise pressure orifices. The spanwise orifices were located along (or near) the trailing edge of each airfoil element to monitor the two-dimensionality of the flow at run time. Integration of the pressure measurements yielded the forces reported here. The data is corrected for the effects of sidewall suction system on the tunnel parameters. Four rows of streamlined support brackets for high-lift devices (Fig. 3) were required due to very high loads (up to 15000 pounds) associated with the high free stream dynamic pressure and lift coefficients obtained. Drag data were computed by integration of static and total pressures obtained from the LTPT wake survey rake system.

RESULTS

Unless otherwise noted, all data are presented for free stream Mach number M = 0.20.

Reynolds Number Effects

The effects of Reynolds number on lift, and maximum lift loss, have been repeatedly documented in the past[1,2,4-6]. The Reynolds number study conducted during this investigation reaffirms the necessity of obtaining measurements at flight-representative Reynolds numbers.

Figure 4 shows the effect of Reynolds number on the multi-element airfoil maximum lift performance degradation, $\Delta C_{\ell,max}$, due to simulated Ice. The data shown indicate that the Reynolds number effect is not large for this case. Previous results, however, show that tests at RN < 5×10^6 are not representative of a flight-scale article[4]. In order to obtain the correct assessment of performance penalties in this complex flowfield, measurements should be obtained as near to the flight Reynolds number as possible. Subsequent results are shown for a Reynolds number of 9 million. This is representative of the full-scale environment that a stall-critical section of a new generation wing on a narrow body twin-jet transport aircraft is expected to experience.

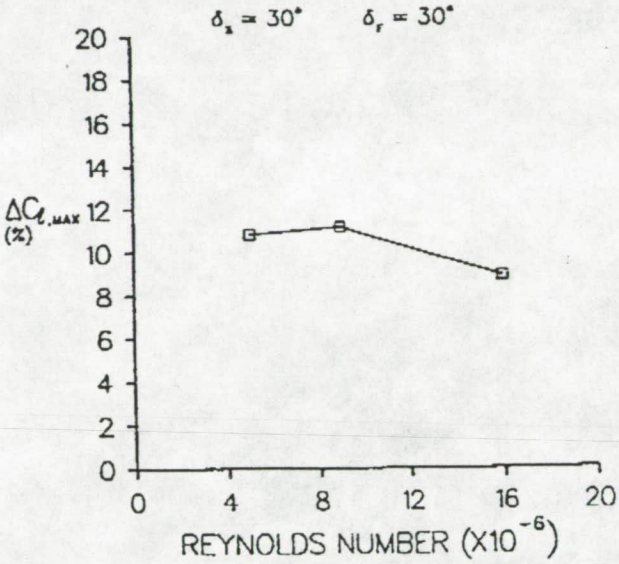

Fig. 4. Reynolds Number Effect on Maximum Lift Loss Due to Simulated Ice Accretion

Iced Airfoil Results - Smooth and Rough

The key objective of this investigation was to assess the performance degradation of a high-lift system in the presence of potential in-flight ice accretions. The lift performance of the multi-element airfoil with ice for RN = 9 million is shown in Fig. 5. The presence of smooth ice accretion on the multi-element airfoil surfaces caused a small drop in $C_{\ell,max}$ with little change in α_{stall}. However, addition of roughness to the ice surfaces caused a substantial loss in airfoil lift performance.

Effects of roughness on airfoil aerodynamics have been long recognized[3-6]. These effects continue to be a source of investigation in iced airfoil aerodynamics. The effect of rough ice is also shown in Fig. 5. The ice roughness was simulated to closely resemble the

measured ice roughness heights in the IRT during icing tests on a similar airfoil[9,10]. Addition of roughness to the simulated ice shape increased the $\Delta C_{\ell,max}$ penalty to over 10%, with reduction of angle-of-attack-margin to stall of nearly 4 degrees. The contribution to the lift deficit comes primarily from the main element, but this is caused by the effect of the slat ice accretion on the downstream elements. The disrupted flow on the slat affects the performance of the main element and the flap. This can be observed from pressure distributions on the three elements of the high lift system.

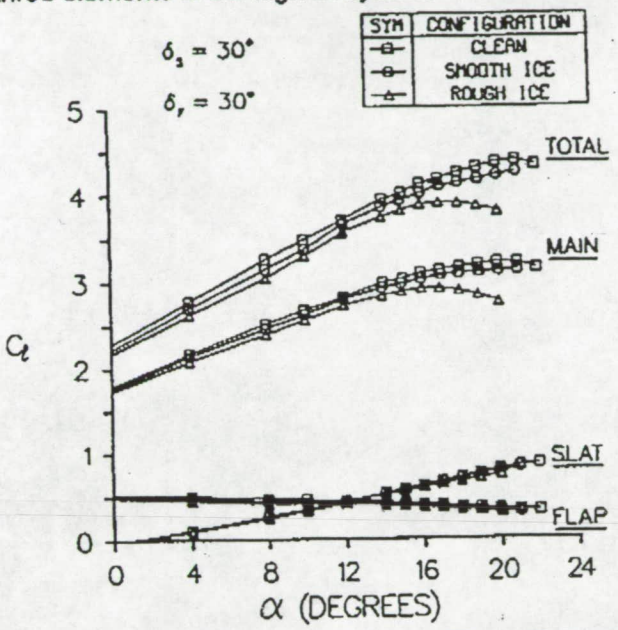

Fig. 5. Effect of Ice on the Lift of a Three-Element Airfoil.

The effect of rough ice on the multi-element airfoil pressure distribution at representative approach conditions is shown in Figs. 6-8 for 9 million Reynolds number. Examination of the pressure distributions indicates that the pressure peaks are reduced on all three elements.

As expected, similar trends are observed near stall. The pressure distributions for the airfoil at α=20 degrees is shown in Figs. 9-11 for the slat, main element and the flap. The drop in the peak Cp's on the three elements is quite evident. There is a pronounced collapse in the slat peak pressure. The influence is felt downstream by the main element and the flap through a reduction in the ability of these elements to maintain the same peak pressures as their respective clean counterparts. Note that the pressure measurements indicate that the presence of rough ice shape[5] on the leading edge of the elements did not produce an appreciable change in the location of the stagnation point in the elements of the high lift system.

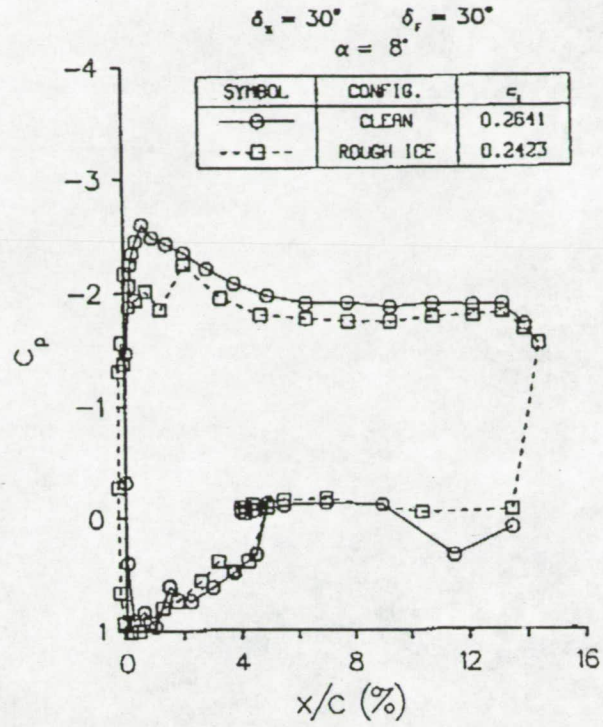

Fig. 6. Effect of Rough Ice on the Slat Surface Pressures at α = 8 degrees

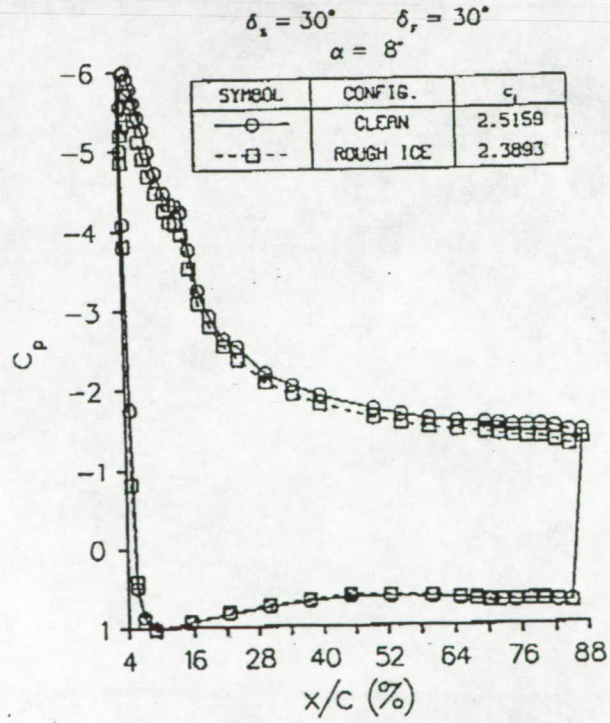

Fig. 7. Effect of Rough Ice on the Main Element Surface Pressures at α = 8 degrees

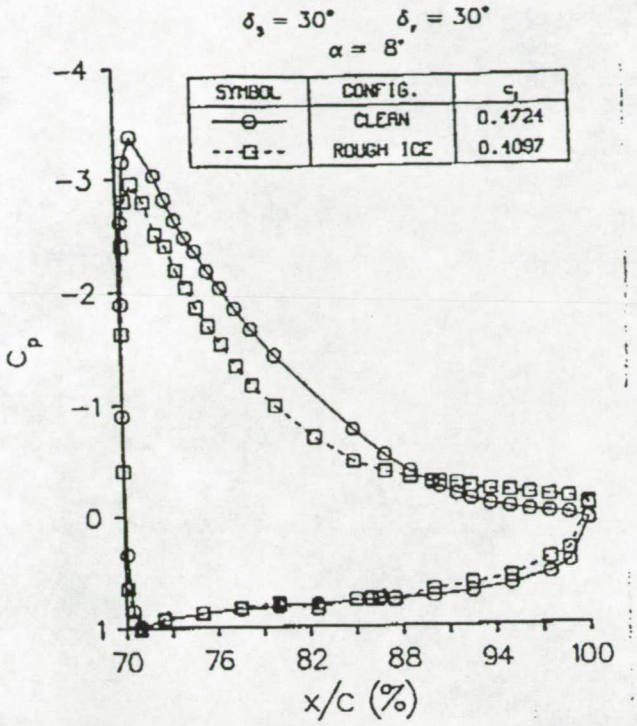

Fig. 8. Effect of Rough Ice on the Flap Surface Pressures at α = 8 degrees

The pressure distributions in Figs. 6-11 demonstrate the effect of rough ice on the peak pressures from each element. The ability to sustain high peak pressures relates directly to the multi-element airfoil's capability to generate high lift. The peak pressure coefficients for the multi-element airfoil are shown in Fig. 12 for RN=9 million. Data are shown for the clean, smooth ice and rough ice configurations. Clearly the rough ice had the most dramatic impact on the peak pressure coefficients. Near stall, growth of the wakes from the slat and main element cause the flap to unload. Unlike the classical mechanisms of stall (involving flow separation), no separation has been observed on the flap at the high angles of attack typical of stall (flap incidence ~ 50 degrees). The growth of the wakes and merging shear layers from the slat and the main element reduce the effective angle of attack experienced by the flap which leads to the flap unloading. This is somewhat analogous to a decambering effect of the airfoil. This in turn leads to the unloading of the aft portion of the main element, and subsequently the unloading of the slat, which can be observed in the peak pressures, as well as the entire pressure distribution.

Presence of ice on the elements of the high-lift system hastens the stall process, and reduces the lift performance in general, by promoting premature growth of the merging wakes and shear layers from the three elements.

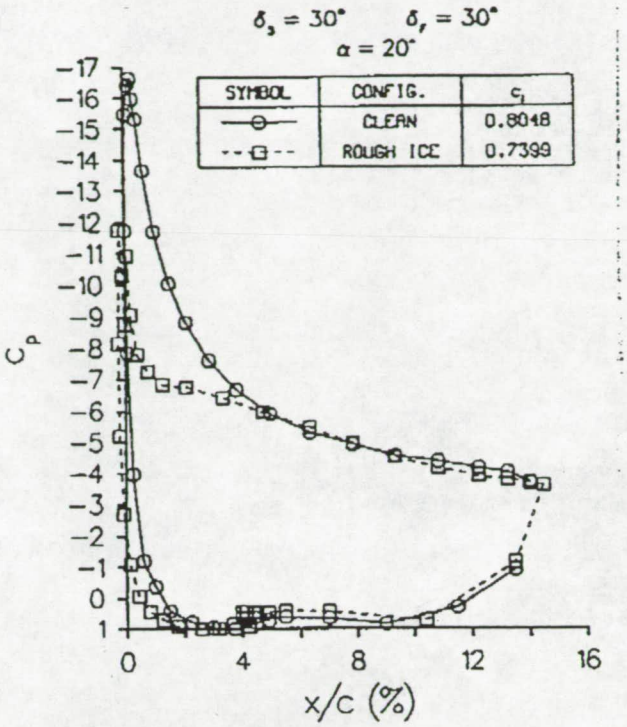

Fig. 9. Effect of Rough Ice on the Slat Surface Pressures at α = 20 degrees

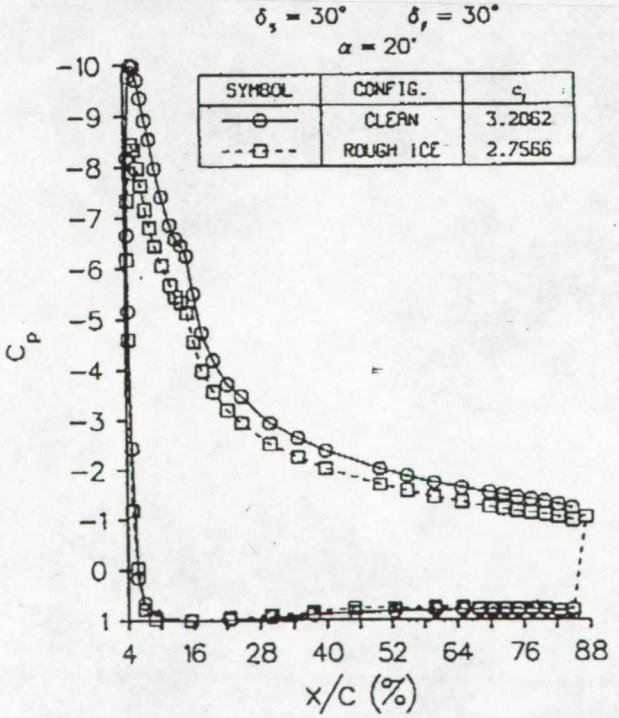

Fig. 10. Effect of Rough Ice on the Main Element Surface Pressures at α =20 degrees

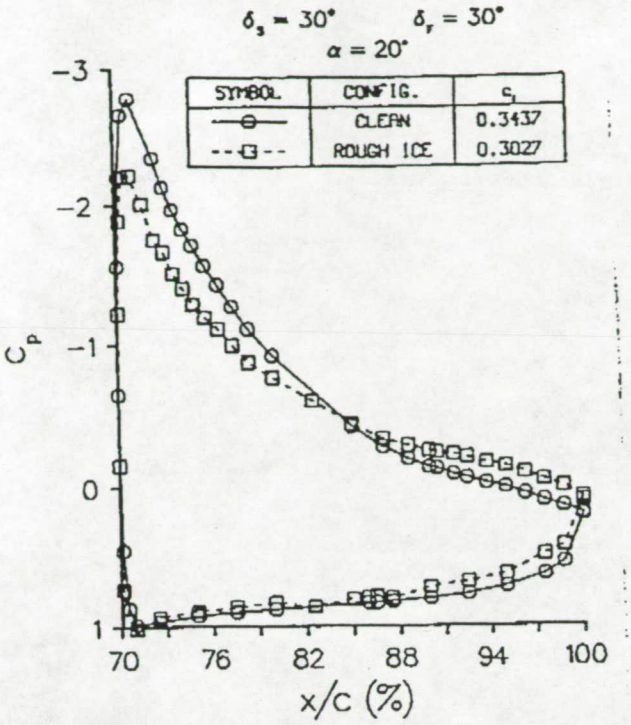

Fig. 11. Effect of Rough Ice on the Flap Surface Pressures at α = 20 degrees

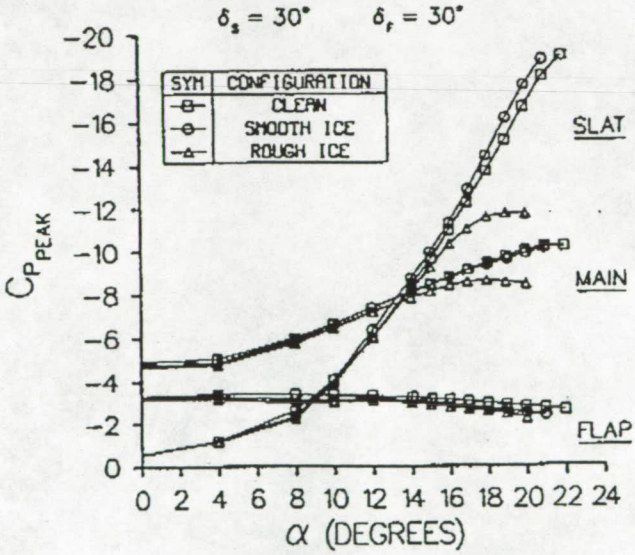

Fig. 12. Effect of Ice on Peak Suction Pressure for a Three-Element Airfoil

In addition to the lift penalty, the presence of ice causes a significant penalty in parasite drag. This is shown for the airfoil at RN=9 million in Fig. 13. The integrated wake rake data showed that the parasite drag nearly doubled at representative approach conditions. All subsequent comparisons with the clean model are presented for the configuration with rough ice.

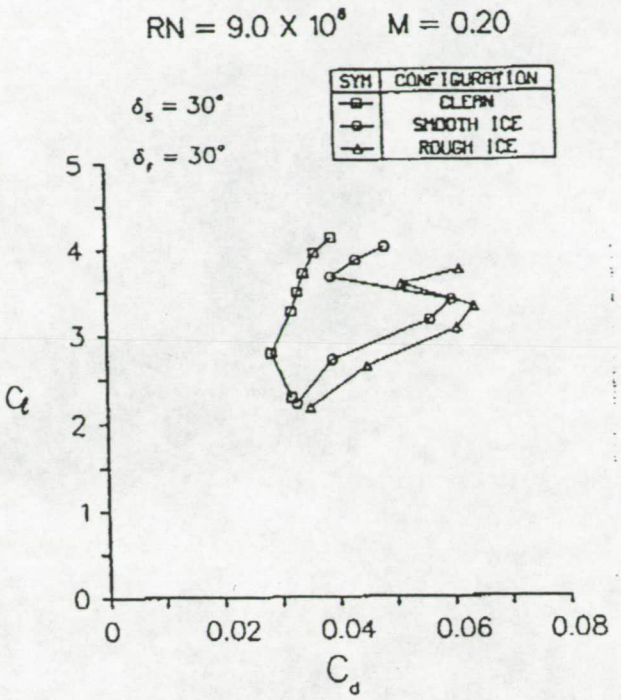

Fig. 13. Effect of Ice on the Drag Performance of a Three-Element Airfoil

Effect of Slat Anti-Ice Operation

The effect of slat anti-ice operation (i.e., keeping the slat free of any ice) on the multi-element airfoil performance was also investigated. This was carried out by testing the three-element airfoil both with and without simulated ice on the slat, with the main element and the flap in the iced configuration. The lift performance of the multi-element airfoil in the landing configuration at RN = 9 million is given in Fig. 14. Data is presented for the clean airfoil along with the following iced airfoil configurations:

a) ice was simulated only on the flap,

b) ice was simulated only on the main element and the flap, and

c) ice was simulated on all three elements.

Recall that for the iced airfoil $\Delta C_{\ell,max}$ was over 10% when all three elements were in the rough-ice configuration. When the slat was kept clean, the $\Delta C_{\ell,max}$ was approximately 4%. Examination of the lift performance data shown in Fig. 14 indicates that contamination of the slat clearly has the largest impact on the lift performance of the high lift configuration tested. This is not unlike the Mach number effect on the

slat performance, where an increase in the free stream Mach number has led to a flow breakdown/limitation which in turn resulted in lift reductions. The loss in $C_{\ell,max}$ and α_{stall} performance due to rough ice on the slat further reinforces the conclusions made following measurements on single- and multi-element airfoils with leading edge roughness[4-6].

Incidentally, the role of the flap in developing and maintaining lift can be observed from the lift performance data shown in Fig. 14. At representative approach conditions (α~8°), the degradation in lift is approximately the same for all configurations shown in Fig. 14. When only the flap was in the iced configuration, the lift increment was somewhat lower than the other iced configurations shown. This suggests that the wake from the flap is altered due to the ice accretion on the flap, which in turn leads to the flap unloading and a reduction in the peak pressures sustained by the flap. As a result, the aft part of the main element and subsequently the slat also unload. Note that this effect is not quite obvious near stall conditions. Here only a small reduction in lift performance is observed when only the flap is iced. Near stall, the flap is mostly unloaded in the clean configuration. Hence, addition of simulated ice to the flap did not result in the same magnitude of lift performance degradation near stall (as it did at representative approach conditions) with no change in angle-of-attack-margin to stall.

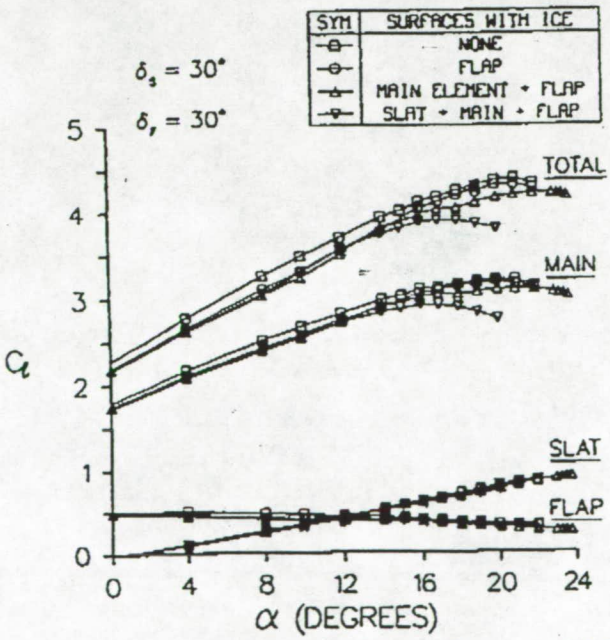

Fig. 14. Lift Performance of a Three-Element Airfoil with Clean and Iced Slat

Although no impact on the stall margin was measured when the slat was clean, a noticeable increase in parasite drag was measured. This is shown in Fig. 15 where the drag polar for the clean multi-element airfoil, as well as the iced configurations, are presented. In general, presence of ice on the multi-element airfoil caused a substantial increase in drag.

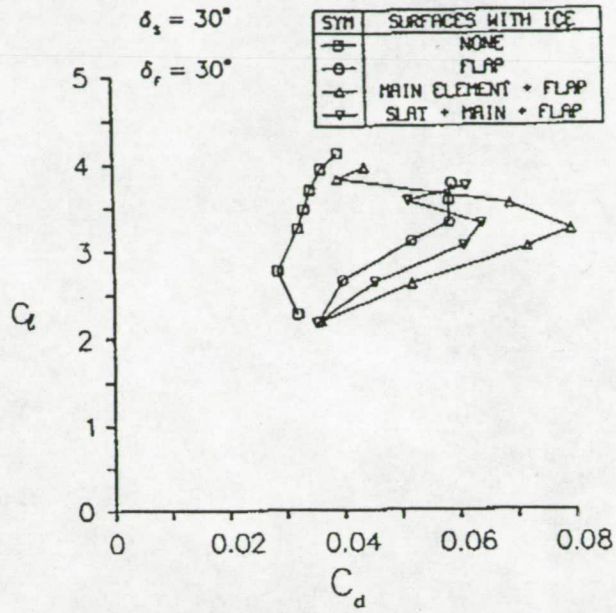

Fig. 15. Drag Performance of a Three-Element Airfoil with Clean and Iced Slat

A typical pressure distribution for the iced airfoil with a clean slat at representative approach conditions is shown in Fig. 16. Regardless of the presence of ice on the slat, none of the high lift elements exhibit the capability to sustain the same peak pressures as their respective clean configuration. It is interesting to note that the drop in slat peak pressure is approximately the same, whether the slat is iced or clean. This clearly indicates the significance of the developing wakes and merging shear layers from the main element (and the flap as mentioned earlier). Regardless of ice on the slat, the premature growth of the main element wake causes the flap to unload, which in turn cause the main element, and subsequently the slat, to drop in peak pressures and normal force in general. Near stall conditions (Fig. 17.), the flap in the clean configuration is already unloaded due to the growth of wakes from the main element and slat. However, the developing wake from the iced slat and the iced main element cause the flap to further unload, thereby reducing the peak pressure sustained by the flap. As mentioned previously, this leads to the main element (and the slat) unloading.

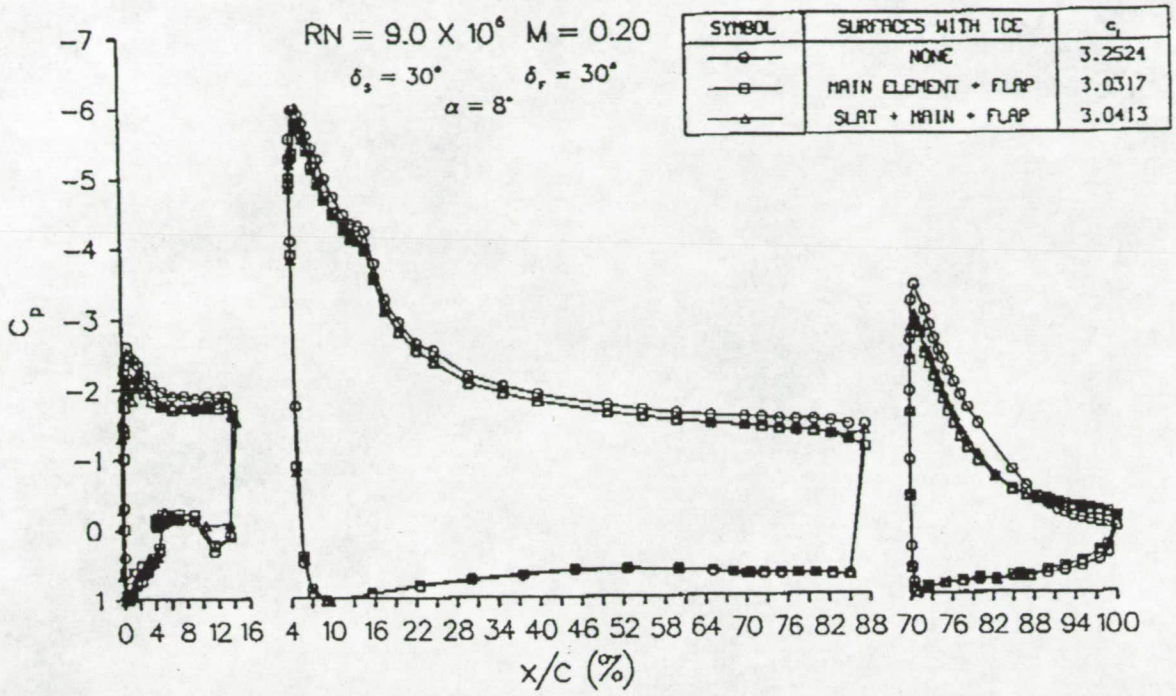

Fig. 16. Surface Pressure Distribution on a Multi-Element Airfoil with Clean and Iced Slat, α = 8 degrees.

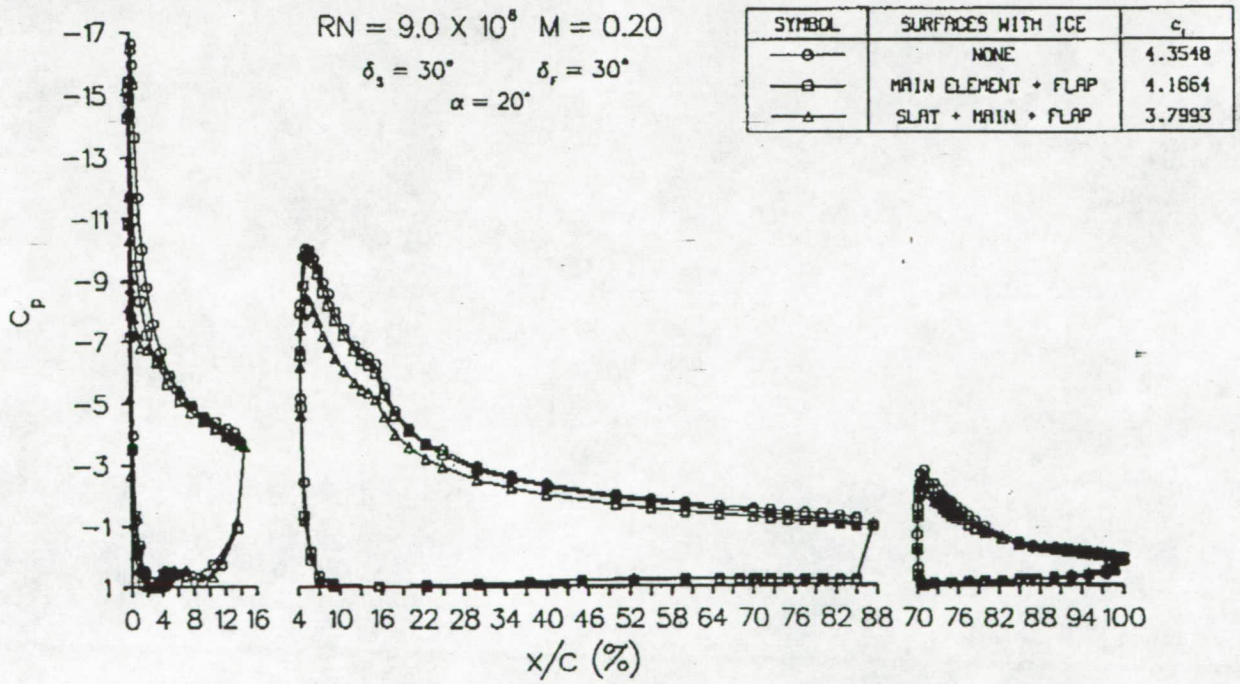

Fig. 17. Surface Pressure Distribution on a Multi-Element Airfoil with Clean and Iced Slat, α = 20 degrees.

** TOTAL PAGE.002 **

CONCLUSIONS

The aerodynamic performance of a multi-element airfoil was evaluated in the presence of simulated ice accretions. The test was conducted at NASA Langley's LTPT at moderate-to-high Reynolds numbers. The ice shapes used were simulations of ice accretions grown on a similar model at the NASA Lewis' IRT. The conditions simulated in the IRT were representative of typical approach conditions for a narrow body twin-jet transport aircraft. Analysis of the results of this investigation has led to the following conclusions:

1. Ice accretion on main element and flap leading edges does not have a significant impact on maximum lift performance. There is no significant loss in angle-of-attack-margin to stall, but there is a noticeable parasite drag increase. These results, and those from prior measurements, point out the critical role that the leading edge of the airfoil plays in maximum lift development. This is true whether the airfoil is single-element or multi-element.

2. The presence of smooth ice accretions on all airfoil surfaces was shown to degrade the $C_{\ell,max}$ and drag performance of the multi-element configuration tested. Addition of roughness to better simulate the actual character of the ice shapes had a large impact on the performance degradation of the iced multi-element airfoil. These results indicated $\Delta C_{\ell,max}$ over 10% accompanied by a reduction of angle of attack margin to stall when roughness was added to the iced surfaces. Prior studies have reported similar magnitudes of performance loss for roughened leading edges of high-lift systems.

The measured performance degradation during this study is based on ice shapes derived from simulation of actual in-flight icing tests conducted in the IRT. Little or no knowledge of the droplet vertical velocity (ie, that associated with down- or up-drafts) which might be present in an actual icing cloud is currently known. Therefore, simulations in ground-based icing facilities (including the IRT) do not account for the vertical velocity of the impinging supercooled droplets that might be present during an icing encounter. This, along with the large turbulence intensity values that are possible in the IRT, leads to speculation that ice accretions on the downstream elements (main element and the flap) may be artifacts of ground-based facility simulation. This possibility must be investigated; although for the present, these results (which may well be conservative) do not indicate any reason to be concerned over losses in stall margin with ice on the main element or the flap.

Results reported in this paper detail the performance losses of an advanced technology multi-element airfoil in the presence of in-flight ice accretion. They represent the first set of performance degradation data known to the authors, in which simulations of realistic ice accretions were tested on a high lift system at flight-scale Reynolds numbers. This effort was a part of a cooperative experimental program conducted by McDonnell Douglas Aerospace, NASA Le[redacted] Research Center, and NASA Langley Resea[redacted] Center to establish a data base of high-lift airfoil[redacted] accretions and their effect on high-lift sys[redacted] performance.

REFERENCES

1. Valarezo, W. O., Dominik, C. J., [redacted] McGhee, R. J., "High Reynolds-Numb[redacted] Configuration Development of a High-Lift Airf[redacted]" AGARD CP-515, paper no. 10, AGARD [redacted] Symposium on High-Lift System Aerodynam[redacted] Banff, Alberta, Oct. 1992.

2. Valarezo, W. O., Dominik, C. J., McG[redacted] R. J., Goodman, W. L. and Paschal, K. B., "M[redacted] Element Airfoil Optimization for Maximum Li[redacted] High Reynolds Numbers," AIAA paper no. 91-33[redacted]

3. Brumby, R.E., "The Effect of Wing [redacted] Contamination on Essential Flight Characterist[redacted] AGARD CP-496, paper no. 2, AGARD [redacted] Specialists' Meeting on Effects of Adverse Wea[redacted] on Aerodynamics," Toulouse, France, 20th April [redacted] May 1991.

4. Lynch, F. T., Valarezo, W. O. and McG[redacted] R. J., "The Adverse Aerodynamic Impact of [redacted] Small Leading-Edge Ice (Roughness) Buildups [redacted] Wings and Tails," AGARD CP-496, paper no. [redacted] AGARD FDP Specialists' Meeting on Effect[redacted] Adverse Weather on Aerodynamics," Toulo[redacted] France, 20th April -1st May 1991.

5. Bragg, M. B., Heinrich, D.C., Vala[redacted] W.O. and McGhee, R.J., "Effect of Underwing [redacted] on a Transport Aircraft Airfoil at Flight Rey[redacted] Number," *Journal of Aircraft*, vol. 31, no. 6, [redacted] Dec. 1994, pp. 1372-1379.

6. Valarezo, W.O., "Topics In Hig[redacted] Aerodynamics," AIAA paper no. 93-3136.

Langley Low-Turbulence Pressure Tunnel," NASA TP-2328, 1984.

8. Paschal, K. B., Goodman, W.L., McGhee, R. J., Walker, B. and Wilcox, P., "Evaluation of Tunnel Sidewall Boundary-Lyaer Control Systems for High-Lift Airfoil Testing," AIAA paper no. 91-3243.

9. Shin, J. , Wilcox, P., Chin, V. and Sheldon, D., "Icing Test Results on an Advanced Two-Dimensional High-Lift Multi-Element Airfoil," AIAA paper no. 94-1869, presented at the 12th AIAA Applied Aerodynamics Conference, Colorado Springs, CO, June 20-22, 1994.

10. Miller, D., Shin, J., Sheldon, D., Khodadoust, A., Wilcox, P., and Langhals, T., "Further Investigations of Icing Effects on an Advanced High-Lift Multi-Element Airfoil, " AIAA paper no. 95-1880, presented at the 13th AIAA Applied Aerodynamics Conference, San Diego, CA, June 19-22, 1995.